Inter-carbon nanotube contact in thermal transport of controlled-morphology polymer nanocomposites

2009 Nanotechnology 20 155702

(http://iopscience.iop.org/0957-4484/20/15/155702)

Nanotechnology **20** (2009) 155702 (10pp) doi:10.1088/0957-4484/20/15/155702

Inter-carbon nanotube contact in thermal transport of controlled-morphology polymer nanocomposites

Hai M Duong[1], Namiko Yamamoto[1], Dimitrios V Papavassiliou[2], Shigeo Maruyama[3] and Brian L Wardle[1]

[1] Department of Aeronautics and Astronautics, Massachusetts Institute of Technology, USA
[2] School of Chemical, Biological and Materials Engineering, University of Oklahoma, USA
[3] Department of Mechanical Engineering, The University of Tokyo, Tokyo, Japan

E-mail: haiduong@mit.edu

Received 31 December 2008, in final form 23 February 2009
Published 25 March 2009
Online at stacks.iop.org/Nano/20/155702

Abstract

Directional thermal conductivities of aligned carbon nanotube (CNT) polymer nanocomposites were calculated using a random walk simulation with and without inter-CNT contact effects. The CNT contact effect has not been explored for its role in thermal transport, and it is shown here to significantly affect the effective transport properties including anisotropy ratios. The primary focus of the paper is on the non-isotropic heat conduction in aligned-CNT polymeric composites, because this geometry is an ideal thermal layer as well as constituting a representative volume element of CNT-reinforced polymer matrices in hybrid advanced composites under development. The effects of CNT orientation, type (single-versus multi-wall), inter-CNT contact, volume fraction and thermal boundary resistance on the effective conductivities of CNT composites are quantified. It is found that when the CNT–CNT thermal contact is taken into account, the maximum effective thermal conductivity of the nanocomposites having their CNTs parallel to the heat flux decreases by ∼4 times and ∼2 times for the single-walled and the multi-walled CNTs, respectively, at 20% CNT volume fraction.

(Some figures in this article are in colour only in the electronic version)

1. Introduction

Carbon nanotubes (CNTs) have been investigated as promising materials for next generation thermal and electrical devices due to their superior thermal, mechanical and electrical properties [1, 2]. Furthermore, aligned CNTs combined with existing advanced composites are being explored for macro-scale aerospace structures that benefit from thermal tailoring and light weight [3, 4]. Accurate thermal transport models within different polymer nanocomposites, and larger-scale complex composites, remain to be developed. Few investigations have focused on the thermal conductivities of aligned CNT-containing composites, and classic models have described the effective thermal conductivity based on microscopic rather than nanoscale considerations. Thermal boundary resistance, playing a dominant role in the determination of the effective conductivities of a composite or a suspension containing high surface-to-volume constituents, needs to be taken into account. As there is no universally accepted analytical solution currently available to accurately predict the thermal conductivity of CNT-containing composites including thermal boundary resistances, it is useful to systematically study the thermal properties of both single-walled and multi-walled CNT composites by numerical methods.

Tomadakis and Sotirchos [5, 6] developed a Monte Carlo algorithm to predict the thermal conductivity of randomly-dispersed cylinders-in-polymer without taking account of the thermal boundary resistance or the ratio of length to diameter of the dispersed phase. Duong *et al* [7, 8] developed a new algorithm by taking into account the thermal boundary resistance at the interfaces between the CNTs and the polymeric matrix. None of the prior work, including Duong *et al*'s work, has considered CNT-to-CNT contact, which

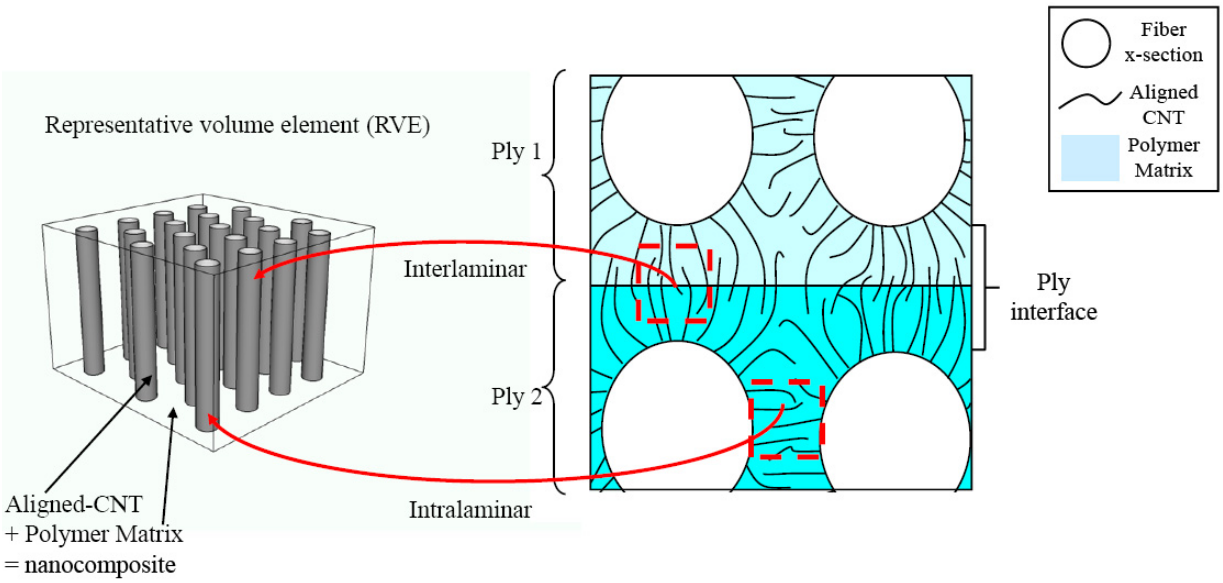

(a)

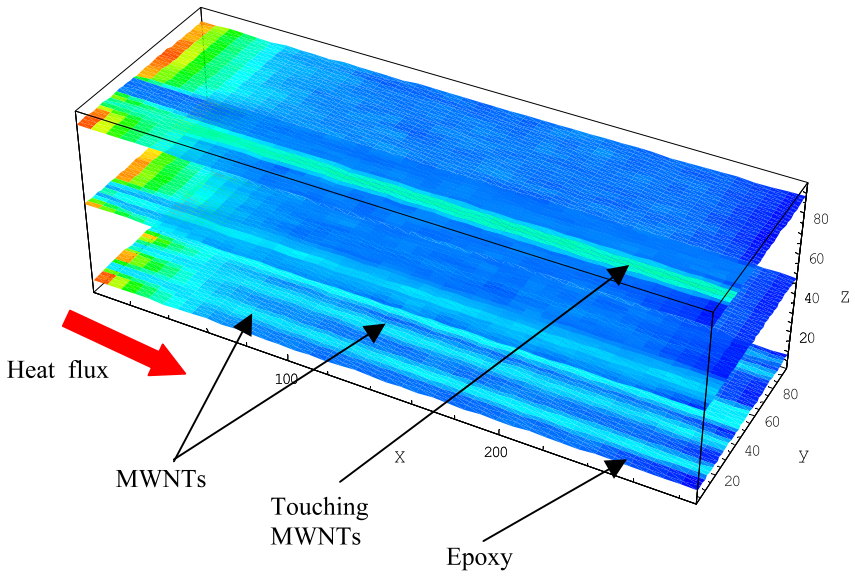

(b)

Figure 1. (a) Schematic drawing of three-phase CNT-reinforced composites, and aligned CNTs in a polymer as a representative volume element and (b) heat distribution of the MWNT-epoxy composite at 20 vol% of the MWNTs parallel to the heat flux at different z positions of the 288 × 96 × 96 grid epoxy cell. The cell is discretized into grid units for temperature evaluation.

is a common occurrence when CNTs form bundles (e.g., sometimes called ropes for single-walled CNTs (SWNTs)) and when SWNTs and multi-walled CNTs (MWNTs) are grown into forests or spun into macroscopic fibers [9], which are wavy and in contact. Several authors have demonstrated that the wavy shape and spatial agglomeration of CNTs have a significant influence on the effective elastic moduli of composites [10–12]. Such effects could potentially modify the thermal properties of CNT nanocomposites, but the case of agglomeration or the case of curved CNT shapes that gives intermittent CNT–CNT contact are not examined in this paper. The random walk approach is utilized to simulate heat transfer through aligned CNTs in line contact with each other (see figure 1(b)), and to study the effect of CNT–CNT heat transfer interactions on the effective thermal transport properties of polymer nanocomposites (PNCs).

In Duong *et al*'s model, resistance to heat transfer at the matrix–CNT interface, known as the Kapitza resistance, is considered explicitly in the prediction of the thermal conductivity of MWNT [7] and SWNT composites [8]. Simulation results have compared favorably with experimental data of SWNT–polymer composites [13, 14]. Since the CNT thermal conductivity is several orders of magnitude larger than the thermal conductivity of the matrix surrounding the CNTs,

Table 1. Parameters used in the simulations.

	SWNT	MWNT
Geometry		
Computational cell size (nm^3)	$300 \times 100 \times 100$	$300 \times 100 \times 100$
CNT diameter (nm)	2.4	8.0
CNT length (nm)	300	300
CNT volume fraction (%)	1, 8, 20	1, 8, 20
Number of CNTs in a cell	22, 179, 448	2[a], 16, 40
Thermal property		
Probability for phonon transmission from matrix to CNT f_{m-CN}	0.02, 0.20, 0.50, 1.00	0.02, 0.20, 0.50, 1.00
Thermal boundary resistance at the CNT–matrix interface, $R_{bd-epoxy}(\times 10^{-8}, m^2\ K\ W^{-1})$[b]	4.36, 0.44, 0.17, 0.09	4.36, 0.44, 0.17, 0.09
Probability for phonon transmission from CNT to CNT f_{CN-CN}[c]	0.0024	0.0024
Thermal boundary resistance at the CNT–CNT interface, $R_{bd-CNT}(\times 10^{-8}, m^2\ K\ W^{-1})$ [11]	24.8	24.8
Thermal conductivity of matrix, K_m ($W\ m^{-1}\ K^{-1}$)	0.2	0.2
Simulation conditions		
Number of walkers	90 000	90 000
Time increment, Δt (ps)	0.25	0.25
Thermal equilibrium factor C_f		
Without CNT–CNT contacts	0.248	0.315
With CNT–CNT contacts	0.230	0.295
Heat flux direction	Parallel and perpendicular to the CNT direction	
CNT–CNT contact	With and without inter-CNT contact	

[a] In this case only, the two MWNTs are forced to be in contact rather than relying on a random assignment.

[b] Thermal boundary resistance R_{bd} is calculated from equation (1); epoxy density is 1.97 g cm^{-3} [26]; epoxy specific heat is 0.97 J $g^{-1}K^{-1}$ [25] and sound velocity is 2400 m s^{-1} [27].

[c] f_{CN-CN} is calculated from equation (1); SWNT density is 1.3 g cm^{-3} [28]; sound velocity in SWNTs is 8000 m s^{-1} [29] and SWNT specific heat is 0.625 J $g^{-1}\ K^{-1}$ [30]. The same f_{CN-CN} value is assumed for the MWNTs due to unavailable experimental data.

the model employs a uniform distribution of thermal walkers inside each CNT, which is equivalent to the assumption of an infinite thermal conductivity of the CNTs relative to the matrix. Typical conductivities for individual CNTs are in the range of 100–5000 W $m^{-1}\ K^{-1}$ whereas typical thermal conductivities for polymers are ~0.2 W $m^{-1}\ K^{-1}$. This algorithm is faster than a molecular dynamics (MD) algorithm and therefore can be used for the simulation of larger domains than those simulated by MD. In comparison to conventional Eulerian methods, such as finite element and finite difference methods, this particle-based and meshless algorithm has the following advantages: (a) there is no need to generate a mesh that would fit the complicated geometry of cylinders dispersed into a matrix material, and to repeat the mesh generation every time a new cylinder configuration is examined; (b) the incorporation of the Kapitza resistance at the CNT–matrix and CNT–CNT interfaces happens in a natural way, through a probability, which is in accordance to the acoustic mismatch theory that describes the Kapitza resistance. As there is no experimental work measuring the thermal boundary resistance across inter-CNT contact, Maruyama *et al* [15] applied molecular dynamics (MD) simulations to estimate the thermal boundary resistance between SWNTs in a bundle. The thermal boundary resistance, R_{bd}, between SWNTs in a bundle was estimated to be 24.8×10^{-8} $m^2\ K\ W^{-1}$ (or the thermal boundary conductance, $K_{bd} = 1/R_{bd} = 4.04$ MW $m^{-2}\ K^{-1}$). Later, Zhong *et al* [16] reported systematic MD studies about the effect of contact morphology on the thermal boundary resistance. The calculated values range between 8×10^{-8} and 11×10^{-8} $m^2\ K\ W^{-1}$, and are slightly smaller than the values of Maruyama *et al* [15]. We used $R_{bd} = 24.8 \times 10^{-8}$ $m^2\ K\ W^{-1}$ calculated for the natural contact morphology of bundles of SWNTs [15]. This value is higher than the other reported boundary resistances 1.0×10^{-8} $m^2\ K\ W^{-1}$ ($K_{bd-PMMA} = 104.9$ MW $m^{-2}\ K^{-1}$) for SWNT–PMMA [8] and 4.3×10^{-8} $m^2\ K\ W^{-1}$ ($K_{bd-epoxy} = 23.4$ MW $m^{-2}\ K^{-1}$) for SWNT-epoxy [8], and it is also higher than the range of matrix–SWNT thermal boundary resistance used for simulations in this work (see table 1).

According to the acoustic theory for the interpretation of thermal resistance [17], the average probability for transmission of phonons across the interface between the carbon nanotubes, f_{CN-CN}, or between the CNT and the matrix, f_{m-CN}, is given by

$$f_{i-CN} = \frac{4}{\rho_i C_i V_{mi} R_{bdi}} \quad (1)$$

where i can be the CNT or matrix; ρ is the density; C is the specific heat; V_m is the velocity of sound and R_{bd} is the thermal boundary resistance.

In order to model the geometrically complex system of CNT-enhanced composites, aligned CNTs in polymer are chosen here as a representative volume element (RVE) for such composites, as shown in figure 1(a). The properties of an RVE of an aligned-CNT nanocomposite must be understood to appropriately model the more complicated 3D hybrid composite. Here, the Duong *et al* [8] model is modified to take into account inter-CNT contact. A primary focus is the non-isotropic heat conduction in aligned-CNT PNCs that are of interest for various heat conducting applications, and also because this geometry constitutes a representative volume element of CNT-reinforced polymer matrices in hybrid advanced composites ('nano-engineered' composites) under development [18]. The resistance to heat transfer at the inter-CNT contact should become important when the matrix material has low thermal conductivity and/or the CNT–matrix interface has a large boundary resistance. The present model is applied for predicting and comparing thermal properties of both SWNT– and MWNT–PNCs of different volume fractions, with and without inter-CNT contact. Random walk simulations of thermal walkers are used to study the effects of the interfacial resistance to heat flow inside the PNCs in the directions parallel and perpendicular to the CNT alignment axis.

2. Simulation algorithm

The computation of the effective transport coefficients is based on an off-lattice Monte Carlo simulation of the motion of a large number of walkers that are carriers of heat and are traveling in a computational cell until steady-state is achieved. The computational domain for the numerical simulation is a rectangular box with CNTs organized in the polymer matrix. The computational cell is heated from one surface (the $x = 0$ plane) with the release of 90 000 hot walkers distributed uniformly on that surface at each time step. Once the walkers contact the PNC edge, they are distributed randomly inside the CNTs and progress into the matrix. The temperature distribution is calculated from the number of walkers found in discretized bins in the domain after steady-state is reached. These bins are used only to count walkers for this calculation; the simulation is meshless. The walkers exit at the surface opposite to the heated surface. The cell is periodic in the other two directions. The walkers move through the matrix material by Brownian motion [19]. The Brownian motion in each space direction is simulated with random jumps that each walker executes at each time step. These jumps take values from a normal distribution with a zero mean and a standard deviation

$$\sigma = \sqrt{2D_m \Delta t} \tag{2}$$

where D_m is the thermal diffusivity of the matrix material and Δt is the time increment. The adequacy of the number of walkers, and of the size of the computational domain, for the calculation of the effective thermal conductivity has been discussed previously [7].

The model assumptions may be summarized as: (1) walkers distribute uniformly once inside the CNTs due to the high CNT thermal conductivity relative to the thermal conductivity of the matrix material; (2) collisions between walkers and thermal boundary resistance between walls inside a MWNT are ignored; (3) the transfer of heat is passive; (4) the thermal boundary resistance is the same for walkers coming in and out of the CNTs; (5) all walkers bounce back when they reach the heated surface; and (6) at the edge boundary of the computational domain, walkers are distributed directly into the CNTs once they contact the top CNT surface.

Once a walker in the matrix reaches the interface between the matrix and a CNT, the walker will move into the CNT with a probability f_{m-CN}, which represents the thermal resistance of the interface, and will stay at the previous position in the matrix with a probability $(1 - f_{m-CN})$. Similarly, once a walker is inside a CNT, the walker will re-distribute randomly within the same CNT with a probability $(1 - f_{CN-m} - f_{CN-CN})$ at the end of a time step, or will distribute randomly in other CNTs in contact with the current CNT with a probability f_{CN-CN} or will cross into the matrix phase with a probability f_{CN-m}. In this latter case, the walker moves first to a point anywhere on the surface of the CNT and then moves into the matrix with a random jump whose magnitude takes values from a normal distribution that has a standard deviation given by equation (2) above.

According to model assumption (4) above, the thermal resistance is the same when a walker moves from one phase into the other, but this does not imply that $f_{m-CN} = f_{CN-m}$. In thermal equilibrium, the average walker density within the CNTs must be equal to that in the matrix at any x-coordinate. Therefore, the exit probability of thermal walkers f_{CN-m} must be weighted such that the flux of walkers into the CNTs equals that going out when they are in equilibrium. The weight factor depends only upon geometry and, to maintain equilibrium, the two probabilities are related as follows [8]:

$$f_{CN-m} = C_f \frac{\sigma A_c}{V_c} f_{m-CN} \tag{3}$$

where A_c and V_c are the surface area and the volume of a CNT respectively; σ is the standard deviation of the random jump in the matrix and C_f is a coefficient that we call the thermal equilibrium factor, which depends on the reinforcement (SWNT and MWNT here) size and shape.

The thermal equilibrium factors C_f of the CNTs used in this work are determined numerically. The random walk algorithm described above was used to simulate thermal equilibrium for the case of a single CNT in the epoxy domain having length $L = 300$ nm and SWNT diameter $D_{SWNT} = 2.4$ nm [20] and MWNT diameter $D_{MWNT} = 8.0$ nm [21]. The computation cell used was $288 \times 32 \times 32$ (cubic grid units) in the x, y and z directions, respectively. One CNT having its axis parallel to the x direction was placed at the computational domain center and thermal walkers were released uniformly (instead of being released at $x = 0$) in the domain and allowed to reach equilibrium. After a simulation time that allows steady-state to be reached, the average walker density within the CNTs should equal that in the matrix. The average

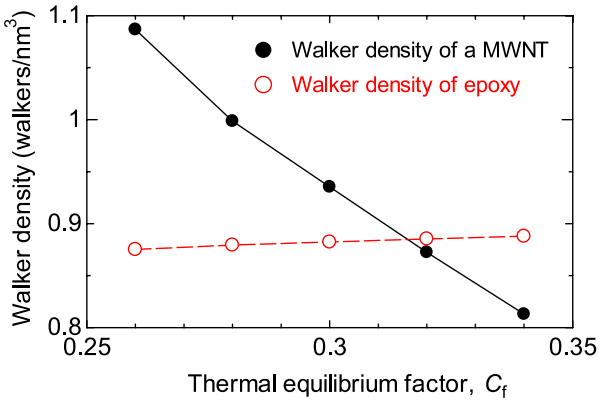

Figure 2. Average walker density of a MWNT (8.0 nm diameter, 300 nm length, 288 grid units) and epoxy with varied thermal equilibrium factor. The value $C_f = 0.315$, where the walker density inside and outside the CNTs is the same, is used in the MWNT in the simulations.

density of walkers inside and outside the MWNT is shown in figure 2 varying with the thermal equilibrium factor C_f. This is a geometry-dependent calculation but is not dependent on the high aspect ratio of CNTs [22]. For the case of CNTs in contact, the C_f was calculated with the same procedure applied to a computational box containing two CNTs in contact along their axis. The C_f values are further confirmed by plotting the walker distribution inside the domain at different positions of the computational cell and ensuring that there are no discontinuities in the distribution. The value of the thermal equilibrium factor C_f is the one resulting in a uniform distribution of the walkers inside and outside of the CNT (see also [8] for more details). In this work, C_f is assumed to be independent of the number of CNTs in contact. In table 1, the appropriate C_f values without the inter-CNT contact are higher than those with the inter-CNT contact.

In order to make the calculation of the effective conductivity more rapid and straightforward, heat transfer with constant heat flux through a domain enclosed between a hot and a cold plane is studied. In this case, the two opposite planes release hot and cold (carrying negative energy) walkers, respectively. Further details of the random walk algorithm can be found in [7, 8]. The input simulation parameters are summarized in table 1. Simulation runs are conducted with different $f_{\mathrm{m-CN}}$, CNT orientation and volume fraction of SWNTs and MWNTs in epoxy. For each CNT orientation in the computational cell and each value of thermal boundary resistance and volume fraction of CNTs, the thermal conductivity is calculated as the average of three simulations with different initial (randomly generated) CNT locations.

3. Simulation results and discussion

3.1. Effects of volume fraction of CNTs and of thermal boundary resistance on the thermal conductivity of the CNT–polymer composites

Heat flow was studied in a 300 × 100 × 100 nm^3 (288 × 96 × 96 grid^3) computational epoxy cell containing CNTS 300 nm in length; 2.4 nm diameter SWNTs or 8.0 nm diameter MWNTs. The CNTs were parallel or perpendicular to the direction of heat flux and extended from one end of the computational domain to the other; in all cases the locations of the CNTs were random. The number of CNTs in the computational cell varied from 22 to 448 (SWNTs) and from 2 to 40 (MWNTs), depending on the volume fraction of CNTs in the epoxy (1–20 vol%). The heat distribution of a MWNT-epoxy composite is shown in figure 1(b) with MWNTs parallel to the heat flux at 20% volume fraction at different positions in the computational cell. The heat distribution in steady-state is shown for three orthogonal slices in the Z-direction; CNT–CNT contact can be observed in the top slice and CNTs without contact can be observed in the bottom slice. The simulations were conducted with different thermal resistances ($f_{\mathrm{m-CN}} = 1.00, 0.50, 0.20, 0.02$, i.e., $R_{\mathrm{bd}} = 0.09$, 0.17, 0.44, $4.36(\times 10^{-8}$, m^2 K W^{-1}), respectively) and with different CNT volume fraction (1, 8 and 20 vol%). The CNT-epoxy thermal boundary resistance values used in this work are less than that of the CNT–CNT boundary resistance of 24.8×10^{-8} m^2 K W^{-1} [15] and fall within the wider range of boundary resistance values considered by Clansy *et al* [23]. The matrix used for the simulations was epoxy with thermal conductivity $K_{\mathrm{epoxy}} = 0.2$ W mK^{-1}.

With and without the inter-CNT contact effects, the thermal conductivities of both the SWNT- and MWNT-epoxy composites having the CNT axis parallel to heat flux are, as expected, much higher than those having CNTs perpendicular to the heat flux, (see figure 3). Similarly, an increased volume fraction of CNTs enhances all the effects of transport whether in the parallel or perpendicular direction with the small thermal boundary resistance. The CNTs span the PNC volume and therefore the PNC conductivity parallel to the CNT axis is dominated by the CNT conductivity, and is only limited by the thermal boundary resistance. Importantly, the R_{bd} of the CNT–matrix interface is the same as that for the ends of the CNTs located at the end of the computational cell. This represents the simplest case and the CNT–domain interface resistance should be further studied and quantified for different thermal interface materials. This explains why the conductivity in figure 3(a) (along the CNT axis) is enhanced at low R_{bd} by the CNTs, but has little effect at high R_{bd} where heat transferred into the CNTs from the matrix becomes vanishingly small and the CNTs act like an excluded volume from a thermal transport perspective. It follows that for the CNT-epoxy composite having CNTs perpendicular to the heat flux, with the CNT volume fraction fixed, the thermal conductivities increase with decreasing thermal boundary resistance. As the boundary resistance decreases, the walkers (i.e., heat) also have higher probability of entering the CNTs and traveling (more quickly) along the radial axis of the CNTs. As the thermal boundary resistance increases (see figure 3(b)), it can dominate the perpendicular transport and a critical value is reached ($\sim 0.5 \times 10^{-8}$ m^2 K W^{-1}) where the CNTs do not enhance thermal conductivity in the composite; and at higher R_{bd}, the CNTs reduce conductivity significantly. A decrease in thermal conductivity below that of the epoxy in the transverse direction may be advantageous

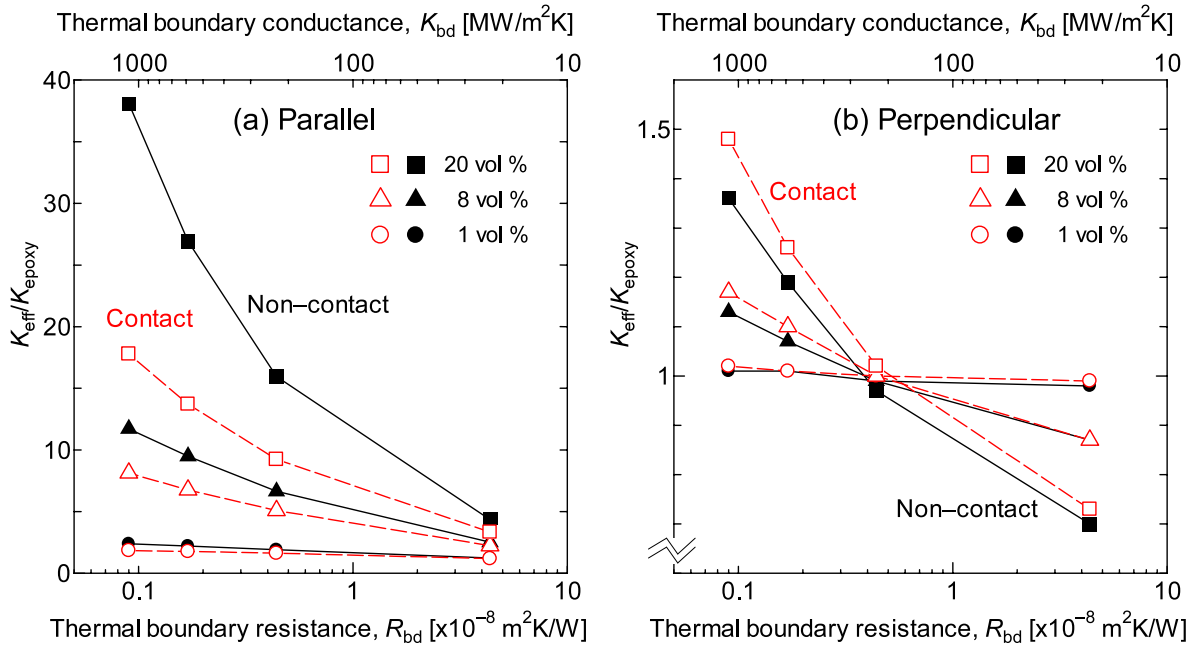

Figure 3. Effective thermal conductivity of MWNT-epoxy composites with MWNTs oriented (a) parallel and (b) perpendicular to the heat flux without (solid dots) and with (open dots) the inter-MWNT contact as a function of thermal boundary resistance with different volume fraction of MWNTs.

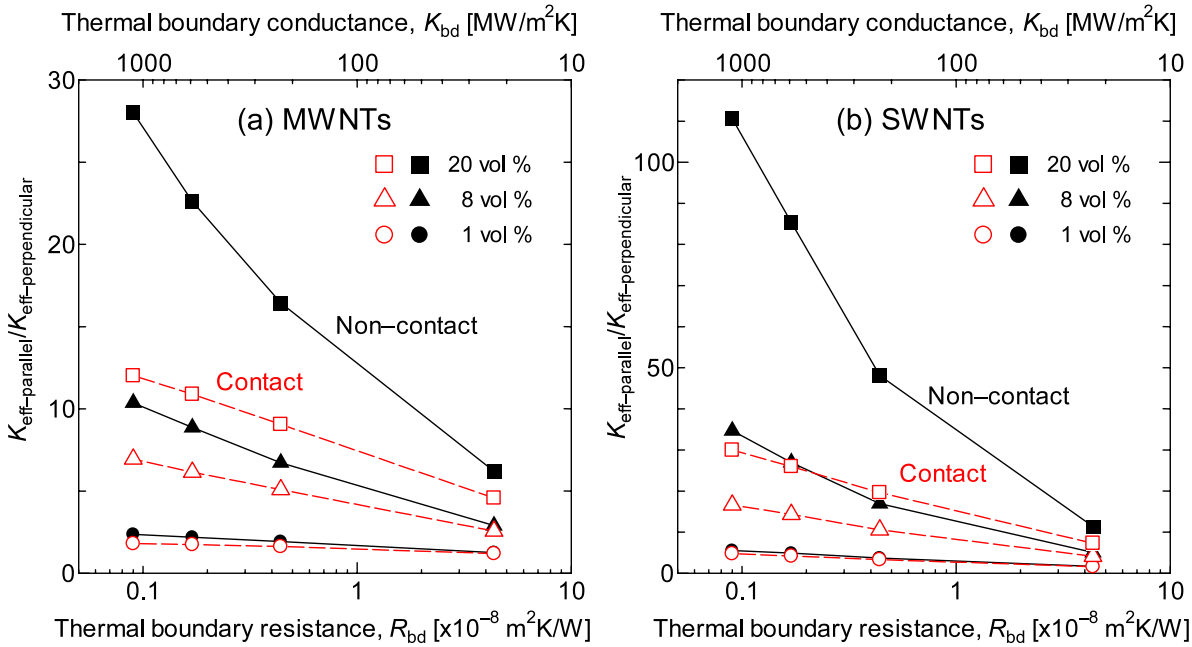

Figure 4. Effective thermal conductivity ratio ($K_{\mathrm{eff-parallel}}/K_{\mathrm{eff-perpendicular}}$) of (a) MWNT- and (b) SWNT-epoxy composites without (solid dots) and with (open dots) the inter-CNT contact effects as a function of thermal boundary resistance with different volume fraction of CNTs.

from a thermal tailoring perspective and is discussed further in relation to figure 4. Note that the thermal conductivity of the PNCs is lower than that calculated from continuum theories that ignore thermal boundary resistances, e.g., the Maxwell theory modified by Rayleigh [24]. According to the simulation results, the maximum thermal conductivity of the MWNT-epoxy composites with 20 vol% is 7.62 W m^{-1} K^{-1}, while the Maxwell theory gives a thermal conductivity of ~600 W m^{-1} K^{-1} (assuming the thermal conductivity of the MWNTs of 3000 W mK^{-1}). The trend in figure 3(b) of decreased perpendicular conductivity with increased CNT volume fraction at high R_{bd} is contrary to predictions by such continuum theories. Thus, depending on the values of the boundary resistance, the trend can agree or disagree with the classical theories, indicating the importance of the thermal boundary resistances and underscoring the need for better experimental quantification of these parameters.

3.2. Effects of inter-CNT contact

The effects of the inter-CNT contact on the effective thermal conductivity of MWNT-epoxy (in figures 3(a) and (b)) and SWNT-epoxy (in figures 6(a) and (b)) are discussed here. When CNTs are parallel to the heat flux, the effective thermal conductivities predicted from the simulations that account for the inter-CNT contact are smaller than those from the model without the inter-CNT contact effect, as shown in figure 3(a). The reasons for this finding are: (1) walkers in the matrix do not see as much CNT surface area to go into when CNTs are touching, and therefore the walkers stay in the matrix longer; and (2) relatively more walkers travel along the CNT radius and cross into adjacent CNTs rather than along the CNT axis, reducing the dispersion of heat in the direction of the heat flux. This is an interesting result that needs to be validated with experimental measurements. Very recent results by Peters *et al* [25] indicate that the thermal conductivity of SWNT–polystyrene composites does not increase with the volume fraction of the CNTs as much as predicted. The reason might very well be the increase of the SWNT–SWNT contact points in the composite, or the value of the CNT–polymer or CNT–CNT thermal boundary resistance. As the CNT–CNT thermal boundary resistance is larger than the CNT–polymer resistance, most of the heat is transferred through CNT–polymer–CNT. Once the CNT–CNT contact is improved, the CNT–CNT thermal boundary resistance is much smaller and the heat transfer through CNT–CNT becomes more important. When CNT–CNT contact is considered in our model, the effective thermal conductivity decreases at a higher rate when the volume fraction of the CNTs increases, or when the thermal boundary resistance decreases, as can be seen, for example, at the point for 20% volume fraction in figure 3(a) (a $\times 2.1$ decrease when CNT–CNT contact is considered).

For the CNTs perpendicular to the heat flux as shown in figure 3(b), with the same thermal boundary resistance and volume fraction of the CNTs, the effective thermal conductivities of the CNT composites when the inter-CNT transfer is taken into account is slightly higher than those without the inter-CNT contact. This is because thermal walkers can now enter through the interface region of the CNT contact and transfer faster along the CNT radius, cross into the next CNTs in contact, and continue along the CNT radius (perpendicular) direction. The inter-CNT contact effect causes significant enhancement of the effective thermal conductivity when the volume fraction of the CNTs increases and the polymer-CNT thermal boundary resistance is low. When the thermal boundary resistance is high, the inter-CNT contact effect causes a significant decrease of the effective thermal conductivity with higher CNT volume fraction. At 20 vol% of the MWNTs and the minimum thermal boundary resistance ($f_{\mathrm{m-CN}} = 1.0$), the effective thermal conductivity of the MWNT-epoxy composites with inter-CNT contact is $\sim$1.1 times higher than that without the CNT contact effect for heat flux perpendicular to the CNTs. It is hypothesized that the effect of CNT–CNT contact is similar to effectively increasing the radius of the CNT: the trends considering CNT–CNT contact in both the parallel and perpendicular directions are directly comparable to the trends observed between SWNT versus MWNT PNCs as discussed subsequently.

The anisotropy ratio of the effective thermal conductivities ($K_{\mathrm{eff-parallel}}/K_{\mathrm{eff-perpendicular}}$) of MWNT- and SWNT-epoxy composites, with CNTs parallel and perpendicular to the heat flux without and with the inter-CNT contact, are shown in figures 4(a) and (b), respectively, as a function of CNT volume fraction and thermal boundary resistance. This anisotropy ratio represents the ratio of the largest to the smallest eigenvalue of the effective thermal conductivity tensor, sometimes called the condition number of the tensor. With the same CNT volume fraction as shown in figure 4(a), the ($K_{\mathrm{eff-parallel}}/K_{\mathrm{eff-perpendicular}}$) ratios of the MWNT-epoxy composites with and without the inter-CNT contact increase at lower values of CNT-epoxy thermal boundary resistance as expected. This trend is significant with higher volume fraction. In all cases the anisotropy ratio is larger than unity, but approaches unity at high values of R_{bd}, where the CNTs act more and more like non-contributing inclusions. CNT–CNT contact effects are noted to follow the same trend in figures 4 as that of increasing CNT diameter. Consider the trend at the lowest value of R_{bd} at 20 vol% fraction where the SWNTs have the highest anisotropy ratio (figure 4(b)), which is reduced substantially if CNT–CNT contact is considered. A similar decrease is noted for MWNTs. The anisotropy ratio also decreases as CNT–CNT contact is allowed for the MWNT in figure 4(a). The effect of CNT–CNT contact is thus noted to be similar to increasing the effective radius of the CNT, diminishing the surface-to-volume ratio of the conductive CNT phase. These trends and observations are consistent with the detailed calculations presented in section 3.3 comparing SWNT and MWNT conductivities.

3.3. Comparison of effective thermal conductivities of SWNT– and MWNT–composites with and without inter-carbon nanotube contact

The ratio of the effective thermal conductivities without the inter-CNT contact effects for SWNT- and MWNT-epoxy composites, normalized by the thermal conductivity of the pure epoxy, is shown in figure 5. Both cases of CNTs oriented parallel and perpendicular to the heat flux are also shown in figure 5. The same type of data, but taking into account the inter-CNT contact, is presented in figure 6. As the CNT volume fraction increases, the thermal conductivity enhancement in the direction parallel to the CNTs is more significant for SWNT-epoxy composites than MWNT-epoxy composites, as seen in figures 6(a) and (b). The maximum thermal conductivity of the SWNT–polymer composite is $\sim$3.5 times and $\sim$2.0 times higher than that of the MWNT-epoxy composite at 20 vol% CNT without and with the inter-CNT contact, respectively. This can be explained because at the same CNT volume fraction, the surface to volume ratio of the SWNTs is higher than that of the MWNTs, and, therefore, the area available for heat transfer between the matrix and the CNTs is higher for SWNTs. Considered in Lagrangian terms, the heat walkers are allowed more chances to come into the CNTs with the same matrix probability and therefore they can move more

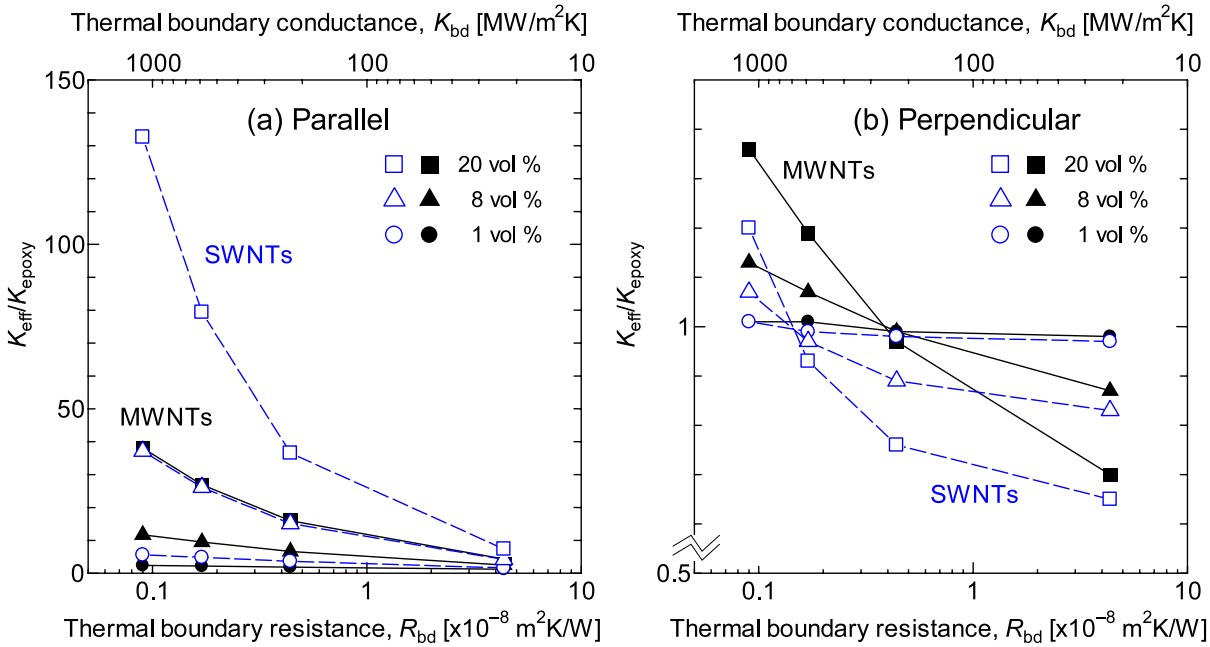

Figure 5. Comparison of effective thermal conductivity of MWNT-epoxy (solid dots) and SWNT-epoxy (open dots) composites with CNTs oriented (a) parallel and (b) perpendicular to the heat flux without the inter-CNT contact as a function of thermal boundary resistance with different volume fraction of CNTs.

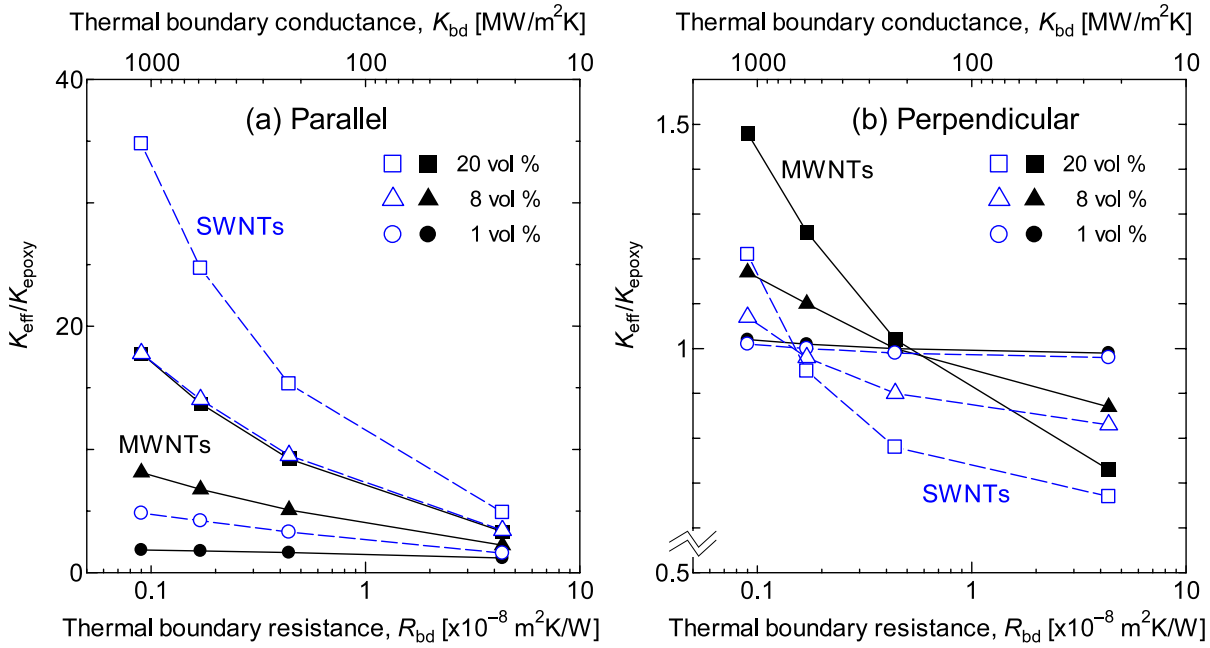

Figure 6. Comparison of effective thermal conductivity of MWNT-epoxy (solid dots) and SWNT-epoxy (open dots) composites with CNTs oriented (a) parallel and (b) perpendicular to the heat flux with the inter-CNT contact as a function of thermal boundary resistance with different volume fraction of CNTs.

rapidly along the direction of the CNT axis. It is apparent that the CNT size plays an important role in the thermal conductivity enhancement. The same reasoning applies for enhanced thermal conductivity with increasing CNT volume fraction. For the CNTs perpendicular to the heat flux as seen in figures 5(b) and 6(b), with the same volume fraction and thermal boundary resistance, the thermal conductivity of the MWNT-epoxy composites is higher than that of the SWNT-epoxy ones. This happens because the larger MWNTs allow more heat to be transferred along their radius. For a relatively small thermal boundary resistance, MWNT-epoxy composites have enhanced conductivity in the perpendicular direction relative to SWNT-epoxy composites. The above observations are consistent with the results both with and without the inter-CNT contact.

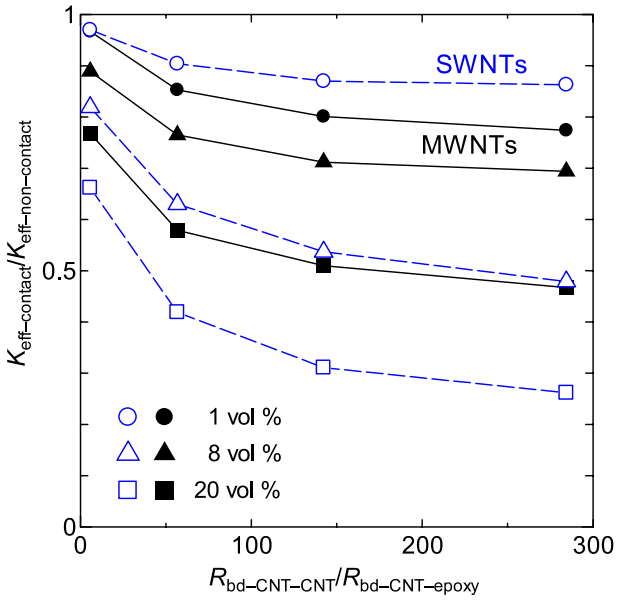

Figure 7. Effect of the relative conductance ratio ($R_{bd-CNT-CNT}/R_{bd-CNT-epoxy}$) on the effective thermal conductivity of a composite when the inter CNT contact resistance is taken into account for MWNT (solid dots) and SWNT (open dots) epoxy composites having the CNT axis parallel to the heat flux direction.

The ratio of effective thermal conductivities, with and without the inter-CNT contact of the MWNT and SWNT composites, as a function of the relative value of the thermal boundary conductances expressed as the ratio ($R_{bd-CNT-CNT}/R_{bd-CNT-epoxy}$) at different CNT volume fractions is shown in figure 7. The CNTs are parallel to the direction of the heat flux, which is the case that yields the maximum effective thermal conductivity. All values of the effective thermal conductivity ratio are less than one, indicating that the resistance to heat transfer at the CNT–CNT contact is reducing K_{eff} for both SWNT and MWNT composites. Furthermore, the higher the difference between the resistance at the CNT–CNT contact and the resistance at the CNT–matrix interface, the larger the reduction of K_{eff}. A high $R_{bd-CNT-CNT}$ effectively prohibits inter-CNT heat exchange, or equivalently, heat transfer is blocked around part of the equivalent radius of the non-contacting CNTs, thereby reducing transport in and out of the CNT relative to the case without CNT contact.

4. Conclusions

A computational model for systematically studying the thermal conductivity of both SWNT– and MWNT–polymer nanocomposites using a random walk algorithm has been developed. This model is more realistic than previous random walk models, because it can take into account the CNT–CNT contact points that are important in high volume fraction CNT composites and in cases where CNTs are in bundles, as in SWNTs. The simulation results show that the maximum thermal conductivity of the CNT composites decreases when there is CNT–CNT contact, for the case where the thermal resistance between CNTs is higher than that between the CNTs and the polymer. This CNT–CNT resistance can dominate thermal transport at very high volume% CNTs. The thermal conductivity of the SWNT composites is higher (parallel to the heat flux case) and less (perpendicular to the heat flux case) than that of MWNT composites under the same simulation conditions, with SWNTs having higher thermal anisotropy ratios than MWNTs at otherwise equivalent simulation conditions. In addition to validating the simulation results with experiments, further research should be conducted to determine (a) the range of thermal resistance for heat transfer between CNTs; (b) the size of this resistance relative to the thermal resistance between CNTs and the matrix material; (c) the degree of intermittent CNT contacts that causes the effective conductivity of the composite to decrease and (d) consideration of other molecules or polymer phases that may exist in synthesized CNTs that will affect the thermal boundary resistances.

Acknowledgments

This work was supported by Airbus SAS, Boeing, Embraer, Lockheed Martin, Saab AB, Spirit AeroSystems, Textron Inc., Composite Systems Technology, and TohoTenax through MIT's Nano-Engineered Composite Aerospace Structures (NECST) Consortium. This work was supported by the National Computational Science Alliance under CTS-040023 and by the TeraGrid under TG-CTS070037T. Namiko Yamamoto acknowledges support from MIT's Linda and Richard (1958) Hardy Fellowship. Dimitrios Papavassiliou acknowledges support from the DoE-funded Center for Applications of Single-Walled Carbon Nanotubes—(Award Register#: ER64239 0012293). Shigeo Maruyama acknowledges support from Grant-in-Aid for Scientific Research (19206024) from the Japan Society for the Promotion of Science, SCOPE (051403009) from the Ministry of Internal Affairs and Communications and NEDO (Japan).

References

[1] Ajayan P M, Schadler L S, Giannaris C and Rubio A 2000 *Adv. Mater.* **12** 750
[2] Choi S U S, Zhang Z G, Yu W, Lockwood F E and Grulke E A 2001 *Appl. Phys. Lett.* **79** 2252
[3] Garcia E J, Wardle B L, Hart J and Slocum A 2008 *Composites* A **39** 1065
[4] Garcia E J, Wardle B L, Hart J, Yamamoto N and Slocum A 2008 *Compos. Sci. Technol.* **68** 2034
[5] Tomadakis M M and Sotirchos S V 1992 *J. Chem. Phys.* **98** 616
[6] Tomadakis M M and Sotirchos S V 1992 *J. Chem. Phys.* **104** 6893
[7] Duong M H, Papavassiliou D V, Mullen J K and Lee L L 2005 *Appl. Phys. Lett.* **87** 013101
[8] Duong M H, Papavassiliou D V, Mullen J K and Maruyama S 2008 *Nanotechnology* **19** 065702
[9] Baughman R H 2000 *Science* **290** 1310
[10] Shi D L, Feng X Q, Huang Y Y, Hwang K C and Gao H 2004 *J. Eng. Mater. Technol.* **126** 250

[11] Fisher F T, Bradshaw R D and Brinson L C 2002 *Appl. Phys. Lett.* **80** 4647
[12] Winey K I, Vaia R A and Guest Editors 2007 *MRS Bull.* **32** 314
[13] Bryning M B, Milkie D E, Kikkawa J M and Yodh A G 2005 *Appl. Phys. Lett.* **87** 161909
[14] Du F, Guthy C, Kashiwagi T, Fischer J E and Winey K I 2006 *J. Polym. Sci.* B **44** 1513
[15] Maruyama S, Igarashi Y, Taniguchi Y and Shiomi J 2006 *J. Therm. Sci. Technol.* **1** 138
[16] Zhong H and Lukes J R 2006 *Phys. Rev.* B **74** 125403
[17] Swartz E T and Pohl R O 1989 *Rev. Mod. Phys.* **61** 605
[18] Wardle B L, Saito D S, Garcia E J, Hart A J and Guzman de Villoria R 2008 *Adv. Mater.* **20** 2707
[19] Einstein A 1905 *Ann. Phys.* **17** 549
[20] Murakami Y, Einarsson E, Edamura T and Maruyama S 2005 *Carbon* **43** 1664
[21] Hart A J 2005 *PhD Thesis* Massachusetts Institute of Technology p 80
[22] Duong H M, Papavassiliou D V, Mullen J K, Wardle B L and Maruyama S 2008 *J. Phys. Chem.* C **112** 19860
[23] Clancy T C and Gate T S 2006 *Polymer* **47** 5990
[24] Bird R B, Stewart W S and Lightfoot E N 2002 *Transport Phenomena* 2nd edn (New York: Wiley)
[25] Peters J E, Papavassiliou D V and Grady B P 2008 *Macromolecules* **41** 7274
[26] Yutopian 2000 *Thermal and Mechanical Properties of Epoxy* June 2008 http://www.yutopian.com/Yuan/prop/Epoxy.html
[27] Bick A and Dorfmueller T 1989 *NATO ASI Ser.* C **291** 389
[28] Collins P G and Phaedon A 2000 *Sci. Am.* 67–9
[29] Hone J, Whitney M and Zettl A 1999 *Synth. Met.* **103** 2499
[30] Hepplestone S P, Ciavarella A M, Janke C and Srivastava G P 2006 *Surf. Sci.* **600** 3633